A Discontinuous Galerkin Method for Variable-Viscosity Stokes Flow

Center for Computational Sciences

JOHANNES GUTENBERG UNIVERSITÄT MAINZ

Ragnar Lehmann[1,2], Boris J.P. Kaus[1,2], Maria Lukáčová-Medvid'ová[1,3]

[1] Center for Computational Sciences, JGU Mainz
[2] Institute for Geosciences, JGU Mainz
[3] Institute of Mathematics, JGU Mainz

Model Problem

We consider different discretizations for Stokes flow on a 2D unit domain $\Omega = [0,1]^2$.

$$-\nabla \cdot \boldsymbol{\tau} + \nabla p = \mathbf{f}, \qquad (1)$$

$$\nabla \cdot \mathbf{v} = 0. \qquad (2)$$

$\boldsymbol{\tau} = 2\mu\dot{\boldsymbol{\epsilon}}(\mathbf{v})$ deviatoric stress, μ viscosity, $\dot{\boldsymbol{\epsilon}}(\mathbf{v}) = \frac{1}{2}(\nabla\mathbf{v} + \nabla\mathbf{v}^\top)$ strain rate, $\mathbf{v}$ velocity, p pressure, $\mathbf{f} = (0, -\rho g)^\top$.

Weak Formulation

Equations (1) and (2) are multiplied with a test function and integrated over each element E of the triangulated domain Ω yielding the weak formulation: Find $(\mathbf{v}_h, p_h) \in \mathbf{V}_h \times P_h$ such that for all $(\mathbf{w}, q) \in \mathbf{V}_h \times P_h$:

$$a(\mathbf{v}_h, \mathbf{w}) + b(\mathbf{w}, p_h) = \int_\Omega \mathbf{f} \cdot \mathbf{w}, \qquad (3)$$

$$b(\mathbf{v}_h, q) = 0. \qquad (4)$$

$\mathbf{V}_h$, P_h: approximation spaces for velocity and pressure, respectively,
$a(\mathbf{v}, \mathbf{w}) = \int_\Omega \nabla\mathbf{w} \colon (2\mu\dot{\boldsymbol{\epsilon}}(\mathbf{v}))$,
$b(\mathbf{v}, q) = -\int_\Omega q \nabla \cdot \mathbf{v}$.

In contrast, the element-wise integration for the Discontinuous Galerkin (DG) method yields additional edge integrals replacing a in (3) by $\tilde{a}$:

$$\tilde{a}(\mathbf{v}, \mathbf{w}) = a(\mathbf{v}, \mathbf{w}) + \sum_e \frac{\sigma}{|e|} \int_e [\mu\mathbf{v}] \cdot [\mathbf{w}] - \sum_e \int_e \{\mathbf{w}\} \cdot [2\mu\dot{\boldsymbol{\epsilon}}(\mathbf{v})]\mathbf{n} - \sum_e \int_e [2\mu\dot{\boldsymbol{\epsilon}}(\mathbf{w})]\mathbf{n} \cdot \{\mathbf{v}\}.$$

E (e) element (edge) of grid, $\mathbf{n}$ unit normal, braces {} average, brackets [] jump of a function on the edge, σ penalty parameter.

H_{DIV} Velocity Spaces

The local (velocity) spaces RT_{k-1} [5] and BDM_k, $k \geq 1$, [1] are composed of weakly divergence-free basis functions. This ensures local mass conservation but requires treatment of jumps across mesh edges.

Remark: With a minor modification of the weak formulation the RT_0 element can resemble the scheme obtained for staggered grid finite differences. [3]

References

[1] F. Brezzi, J. Douglas, Jr., and L.D. Marini, Two Families of Mixed Finite Elements for Second Order Elliptic Problems, 1985.

[2] T. Gerya, Introduction to Numerical Geodynamic Modelling, 2010.

[3] G. Kanschat, Divergence-free discontinuous Galerkin schemes for the Stokes equations and the MAC scheme, 2008.

[4] H. Ramberg, Instability of Layered Systems in the Field of Gravity, 1968.

[5] P.A. Raviart, J.M. Thomas, A mixed finite element method for 2-nd order elliptic problems, 1977.

[6] S. Zhong, Analytic solutions for Stokes' flow with lateral variations in viscosity, 1996.

Element Overview

Location of Degrees of Freedom (DOF):

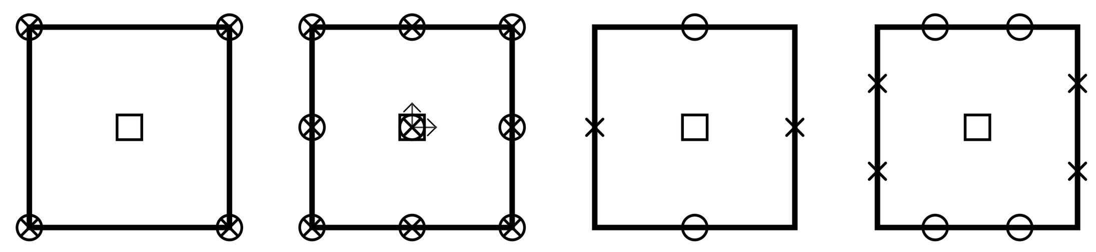

Figure 1: DOFs for Q_1–P_0, Q_2–P_1, RT_0–P_0, BDM_1–P_0.

Square, X, circle denotes pressure, horizontal and vertical velocity DOF, respectively. Arrows denote pressure gradients.

For the RT_0 and BDM_1 elements the horizontal (velocity) component is continuous in horizontal direction and discontinuous in vertical direction, the vertical component vice versa.

Results

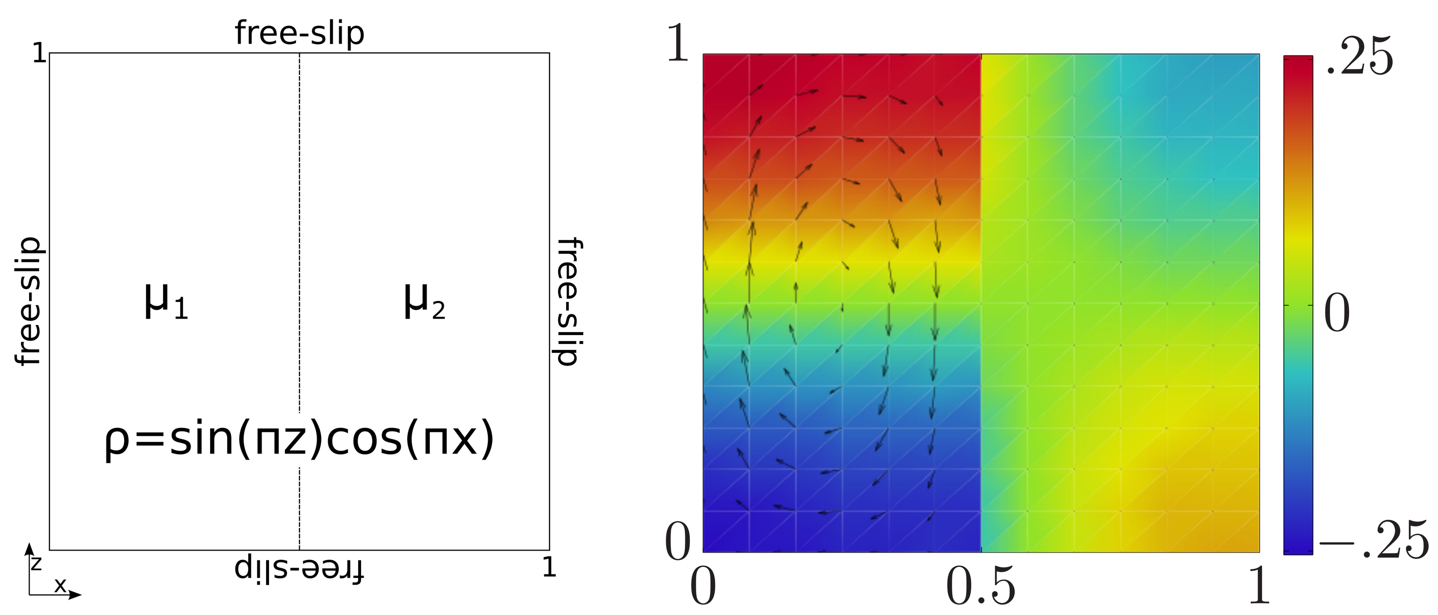

Figure 2: Benchmark setup with lateral viscosity jump. Analytical velocity (arrows) and pressure (colorbar) solution for $\mu_1 = 1$, $\mu_2 = 10^3$.

Benchmark with lateral viscosity jump and free-slip boundaries [6], $\mathbf{f} = (0, \sin(z\pi)\cos(x\pi))^\top$. It has been computed for $\mu_1 = \mu_2 = 1$ and for $\mu_1 = 1$, $\mu_2 = 10^3$, see Fig. 3. As the Raviart-Thomas element does not lead to convergence for discontinuous viscosity, its plot is omitted for the variable viscosity setup.

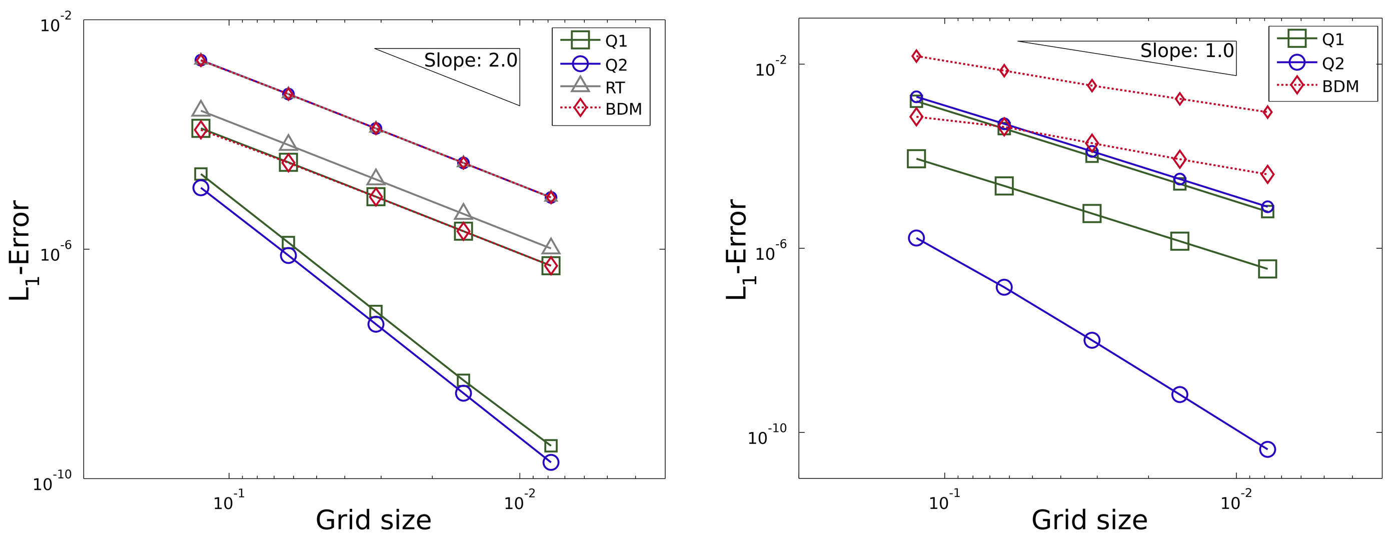

Figure 3: L_1 errors of the four elements for velocity (large markers) and pressure (small markers) for the isoviscous setup (left, $\mu_1 = \mu_2 = 1$) and the variable viscosity setup (right, $\mu_1 = 1$, $\mu_2 = 10^3$).

Element	DOFs	NNZ
Q_1–P_0	3202	47 830
Q_2–P_1	11 522	307 216
RT_0–P_0	3136	26 428
BDM_1–P_0	5248	201 456

Number of global degrees of freedom and number of non-zero entries in the system matrix for the four elements on a square 32-by-32-mesh.

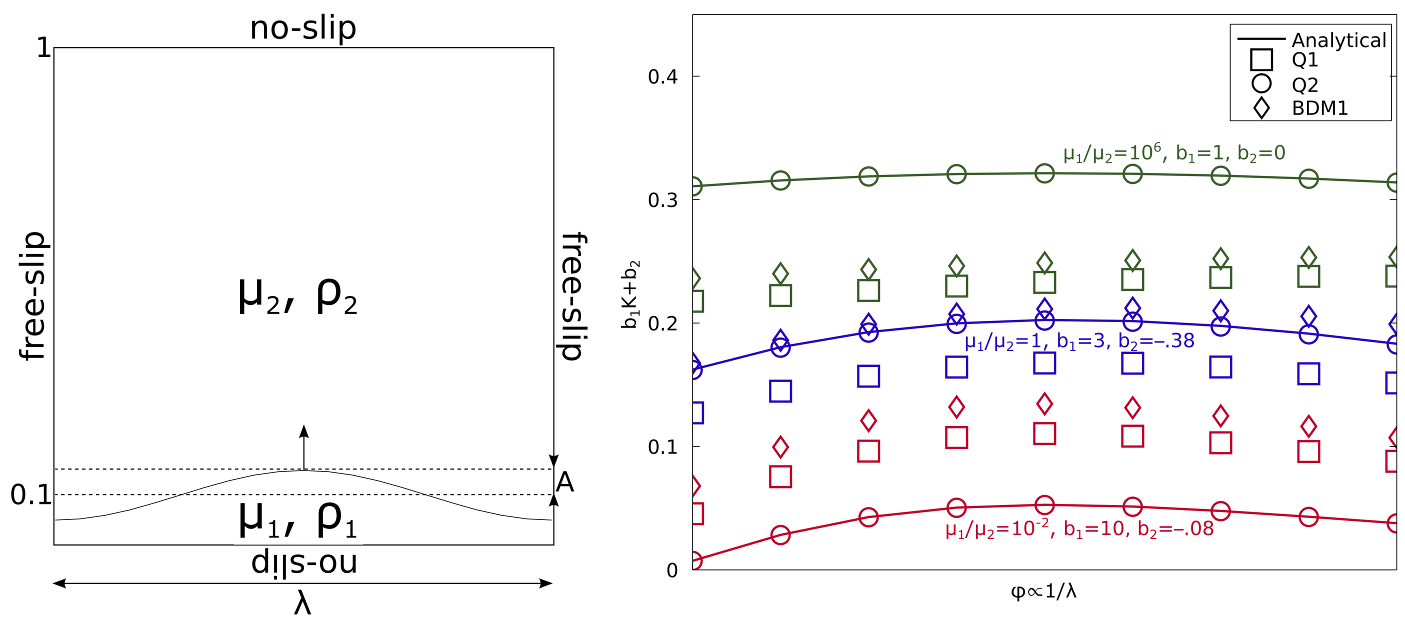

Figure 4: Benchmark setup for Rayleigh-Taylor instability. The jump in density and viscosity is following a small perturbation of amplitude A at $z = 0.1$. For different viscosity contrasts and wavelengths λ the growth factor K has been computed. b_1, b_2 have been chosen such that the plots fit into one figure.

Rayleigh-Taylor instability benchmark with vertical free-slip and horizontal no-slip boundaries [4, 2]. The flow is driven by the density difference $\rho_2 - \rho_1$ (normalized to 1). The mesh edge at $z = 0.1$ is perturbed in a cosine shape with amplitude $A = 10^{-4}$. As above the Raviart-Thomas element is omitted.

Conclusions

- The discontinuous RT_0–P_0 approximation is a very economical element reaching its limitations where viscosity jumps occur.
- The BDM_1–P_0 element is comparable to the (unstable) Q_1–P_0 element, outruns in it some setups in terms of accuracy without getting computationally as expensive as the Q_2–P_1 element.